Ion trajectories in quadrupole mass spectrometer with a static transverse magnetic field applied to mass filter

B.Srigengan, J.R.Gibson and S.Taylor

Abstract: An experimental study has been carried out using a quadrupole mass spectrometer (QMS) in which a static magnetic field is applied transversely to the body of the filter. These results have been compared with theoretical mass spectra obtained by computing the trajectories of all injected ions using the local field conditions. Significant improvement in QMS resolution may be obtained under certain magnetic field conditions, and these have been identified and explained in terms of the theoretical model.

1 Introduction

Quadrupole mass spectrometers (QMS) have found a wide range of applications in the medical field and chemical and biochemical sectors for elemental and isotopic analysis. A good general review of quadrupole mass spectrometry is given in Dawson [1]. More recently the improved performance of miniature mass spectrometers has generated interest in their use in residual gas analysis and as process monitoring devices in semiconductor fabrication plants [2, 3]. The requirement of an application sets the value of resolution, sensitivity and stability of operation which depend on operating conditions of the ion source and the filter.

There have been numerous attempts to theoretically model the performance of the quadrupole mass filter: as an introduction for the work presented here we would refer the reader to [1, 4–11]. Some workers have used an analytical approach to model ion transmission through the filter by calculating ion trajectories in exactly determined hyperbolic quadrupole fields [4, 5]. This analysis has also been applied in other stability regions [6]. Other workers have used commercially available software tools, such as SIMION 3D, to compute field conditions and ion trajectories for the real case i.e. a finite length quadrupole field with circular electrodes [7]. Another approach has been to numerically compute the trajectories of every ion passing through the mass filter [8]. The dependence of ion transmission on the AC phase and the effect of waveform harmonics have been investigated using this approach [9, 10]. Recently this method has been extended to allow the simulation of theoretical mass spectra by the computation of the trajectories of large number of ions (up to 10^6) injected into the quadrupole at each point on the mass scale [11].

Usually QMS resolution can be improved by increasing the number of AC cycles of the alternating field experienced by the ions when passing through the mass filter. This may be achieved by increasing the quadrupole rod length, or increasing AC operating frequency or reducing the ion energy. Electron multipliers can be used to increase sensitivity by detecting very low ion currents (~10^{-16}–10^{-19}A). Modifications to improve performance increase the cost of the instrument. If an alternative method can be found to improve aspects of performance at lower cost then this would be of interest and is one of the motivations behind this study.

The use of magnetic fields in quadrupole ion sources, ion traps and in larger magnetic sector instruments is well known. However, surprisingly little work has been done concerning the application of magnetic fields to QMS mass filters. Poritsky and Gerrard [12] provide an exact analytical solution for the case of electron motion in a quadrupole electric field with a static magnetic field applied in the direction of the z-axis. However, in their case the electric field was not time varying as is the general case for the QMS. In an analytical study Pavlenko and Toporoba [13] considered ion motion in a homogeneous magnetic field. They showed that by varying the magnetic field: (i) resolution could be increased, and (ii) it is theoretically possible to operate the QMS in any Mathieu stability region. Independently of these studies we found experimentally that the application of a magnetic field improved QMS resolution by reducing the well known 'long tail' on the low-mass side of the spectra. Our original numerical model [9] was modified to include the effect of a transverse magnetic field and predicted a resolution improvement depending on the orientation of the field with respect to the mass filter electrodes [14]. In this paper therefore we extend that previous work and present new experimental results of QMS operation under a static transverse magnetic field for a range of operating conditions and masses.

2 Experimental

A conventional 5 inch long QMS with 0.25 inch diameter rods excited at 4MHz and operated with a hot filament ion source and Faraday detector was used. The system was housed in a stainless steel vacuum chamber pumped by an oil diffusion pump, backed by a rotary backing pump providing a residual gas pressure of 2×10^{-7} torr. During the experiments an Ar/air gas mixture was leaked into the vacuum chamber, raising the working pressure to about 3×10^{-6} torr. A transverse magnetic field was applied along

IEE Proceedings online no. 20000815

DOI: 10.1049/ip-smt:20000815

Paper first received 28th March and in revised form 7th September 2000

The authors are with the Department of Electrical Engineering and Electronics, Brownlow Hill, University of Liverpool, Liverpool L69 3GJ, UK

the length of the mass filter using a permanent magnet arrangement and measured using a Hall effect sensor. The value of the magnetic flux density in all cases was 0.017T. The resolution was adjusted by varying the DC to AC voltage ratio (U/V) so as to increase the slope of the scan line towards 100%, where 100% corresponds to the intersection of the scan line with the peak of the Mathieu stability diagram at $U/V = 0.168$ [1]. Following previous theoretical work [14], the magnetic field was applied along the x-axis of the QMS mass filter. The time varying electrostatic field applied to the electrodes aligned in this direction was $U - V \cos 2\pi ft$, where f is the AC excitation frequency (4MHz). The ion energy was set at 20eV to give a measurable ion current at high resolution.

The QMS electronic drive unit was fully automated and driven by a PC to scan the mass filter electrode voltages. The PC also recorded the detected ion current, which was amplified by an electrometer and converted to digital form using a 12-bit ADC. To increase the signal to noise ratio, the ion current signal from the Faraday detector was collected at individual mass values and averaged. Start mass, end mass (range), number of steps, sweep rate and averaging were user selected. A visual display of each mass scan was also displayed in real time on the PC.

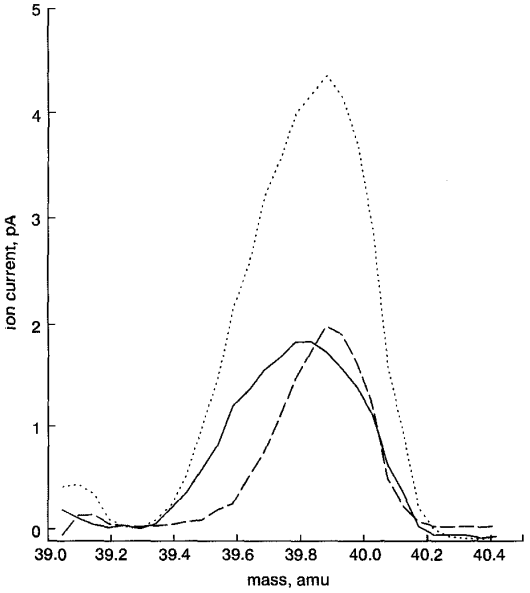

Fig. 1 *Experimental mass spectra of Ar^+ without application of a magnetic field ($B = 0$) for three different ion source emission currents and for low and high resolution R*
——— 100μA, low R
····· 1mA, low R
– – – – 1mA, high R

3 Results and discussion

To demonstrate the basic effect of the magnetic field, Ar^+ spectra were obtained with and without the magnetic field, B, applied. Fig. 1 shows typical spectra obtained from the QMS for electron emission currents (I_e) from the ion source filament of 0.1 and 1.0mA for two different values of U/V ratio. The increased emission current results in increased ionisation in the source and increased ions injected into the mass filter with correspondingly increased ion current in the detector. These results are readily explained in terms of the usual trade-off between decreasing ion transmission and increasing resolution of the instrument as the resolution (U/V ratio) is increased towards the maximum value. Fig. 2 shows the results for the same experimental conditions except for the application of a transverse magnetic field of 0.017T across the body of the mass filter. Three observations may be made:

(i) There is an improvement in resolution (defined as $M/\Delta M$ at 10% peak height) in all cases in which the magnetic field is applied.

(ii) The resolution improvement arises from a reduction in peak width with applied magnetic field which occurs on the low-mass tail of the mass spectra.

(iii) There is an enhancement of ion current transmitted by the QMS in the case of the applied magnetic field for both resolution settings when $I_e = 1$ mA.

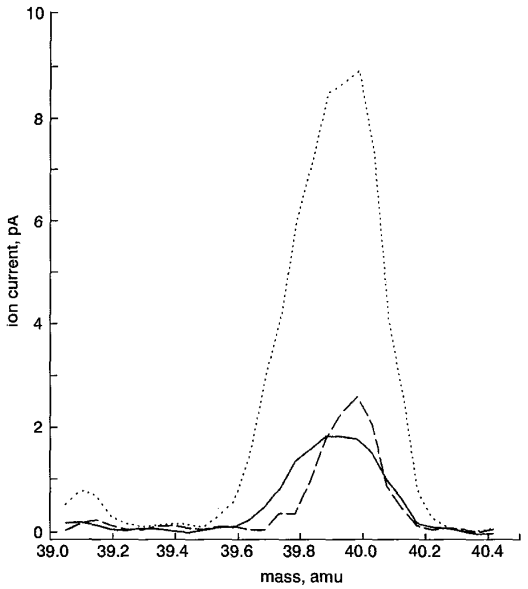

Fig. 2 *Mass spectra of Ar^+ with a magnetic field applied ($B = 0.017T$) for the same experimental conditions as in Fig. 1*
——— 100μA, low R
····· 1mA, low R
– – – – 1mA, high R

Observations (i) and (ii) may be explained as follows: it has been previously shown that on the low-mass side of a mass spectrum the ions which are rejected from the filter have ion trajectories unstable in the x-direction [1]. By tracing the trajectories of a large number of ions injected into the mass filter from their origin in the source we were able to produce contour maps showing that on the low-mass side of the mass spectra such ions originate close to the x-axis [11]. These ions exhibit little (if any) motion in the y-direction. Similarly, on the high-mass side of the spectra, ions rejected from the filter are unstable in the y-direction and these originate close to the y-axis of the mass filter. Results close to the peak of a mass spectrum indicate that ions originate with no bias towards proximity to a particular axis in the source plane. For ions in the low-mass tail, originating close to the x-axis, the application of a magnetic field to the mass filter in a direction perpendicular to the direction of ion motion causes a Lorentz force ($B_x \; x \; v_z$) which results in an increased instability. Such ions are therefore rejected from the mass filter, reducing the width of mass spectrum and thus increasing the resolution. Owing to the asymmetric nature of the mass spectrum peak, in the converse case for ions originating close to the y-axis, the Lorentz force ($B_y \; x \; v_z$) has little effect. Observation (iii) is not thought to be due to any modification of ion transmission in the body of the mass filter but rather due to leakage flux from the permanent magnet affecting the ion source.

A small amount of leakage flux into the source would cause increased electron path lengths resulting in increased ionisation and increased numbers of ions injected into the mass filter for a given electron emission current.

3.1 Theoretical simulation

To confirm hypotheses (i) and (ii) above, the simulation programme described in [11] was adapted to include the magnetic field terms. The equations of motion for an ion in a conventional QMS with hyperbolic electrodes is usually given in dimensionless form ([1], p.13) and separately describe the ion motion in orthogonal directions. Addition of a transverse magnetic field couples the three equations as:

$$\frac{d^2x}{d\xi^2} = -x(a - 2q\cos 2\xi) + \left(\frac{dy}{d\xi}b_3 - \frac{dz}{d\xi}b_2\right) \quad (1)$$

$$\frac{d^2y}{d\xi^2} = y(a - 2q\cos 2\xi) + \left(\frac{dz}{d\xi}b_1 - \frac{dx}{d\xi}b_3\right) \quad (2)$$

$$\frac{d^2z}{d\xi^2} = \left(\frac{dx}{d\xi}b_2 - \frac{dy}{d\xi}b_1\right) \quad (3)$$

with parameters defined as in the Appendix.

The programme operates by dividing the ion trajectory into small steps and assumes that over the step the motions in the three directions x, y and z may be uncoupled. Mass scans are computed by setting a resolution defined by fixing U/V and then varying V. At each value of V a large number of ions are generated (typically over 10^5) and V defines the mass scale in the simulation. Ions are generated at random at any point in the QMS entrance aperture and at times that are random with respect to the AC voltage applied to the QMS rods. Fig. 3 shows three simulated spectra for Ar^+ (mass 40) ions for the experimental system described above. The simulation is for a medium resolution case with ion energy of 20eV and U/V = 98.4% to better illustrate the effect. For the scans a small ion energy spread (about 3eV FWHM) and a small angular spread on ion entrance into the mass filter of 5° half-angle was assumed. Curves (i) and (iii) show the spectra for the case of $\boldsymbol{B}$ = 0 and $\boldsymbol{B}$ = 0.017T applied in the y-direction. The curves are almost indistinguishable on the scale shown and equal when the scatter of random ions is taken into account indicating that the magnetic field has negligible effect. Curve (ii) shows the resulting spectrum with $\boldsymbol{B}$ = 0.017T applied in the x-direction. An increase in resolution is clearly seen at the expense of a 50% reduction in the number of ions transmitted.

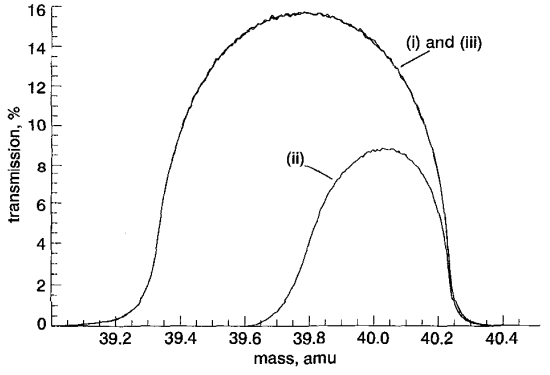

Fig. 3 *Simulated mass spectra for Ar^+ ions showing percentage transmission for three cases*
(i) $\boldsymbol{B}$ = 0; (ii) $\boldsymbol{B}_x$ = 0.017T; (iii) $\boldsymbol{B}_y$ = 0.017T

We consider now some individual ion trajectories with and without the magnetic field applied. Figs. 4–6 show the trajectories for ions transmitted with and without magnetic field applied. The corresponding traces are for ions injected into the mass filter at the same point in time (AC phase) and space and at the same point on the mass scale (m = 39.8amu). In each Figure the upper trace is always for the case of no applied field and the lower trace is for $\boldsymbol{B}_x$ = 0.017T. For Fig. 4 the ion originates at x = 0.1mm, y = 0.0 and the AC phase on entry is 0. Because y = 0 on entry, the electric field in the y-direction $\boldsymbol{E}_y$ = 0 and the ion does not move in the y-direction. The ion is always at y = 0.0 in the upper trace. In the lower trace of Fig. 4 the Lorentz force, $\boldsymbol{B}_x \boldsymbol{x} \boldsymbol{v}_z$ moves the ion away from y = 0.0 and the ion starts to oscillate in the $\boldsymbol{E}_y$ field. The effect of $\boldsymbol{B}$ therefore is to shift the ion motion in the y-direction with respect to the QMS axis. In Fig. 5 the ion originates at x = 0.01mm,

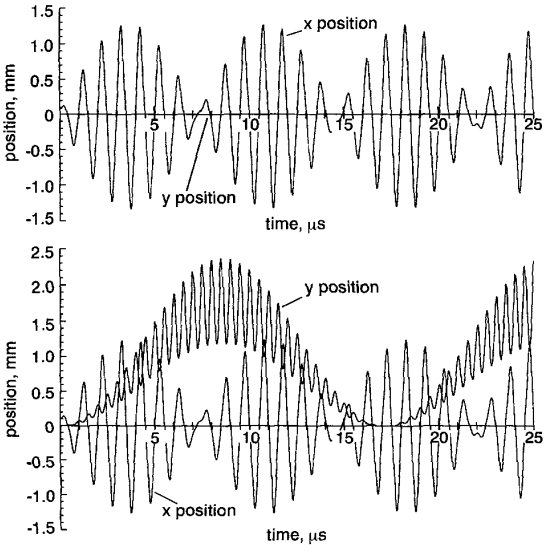

Fig. 4 *Numerical simulation of ion trajectories in x and y for Ar^+ without $\boldsymbol{B}$ (upper trace) and with $\boldsymbol{B}$ (lower trace)*
Point of entry in both cases: x = 0.1 mm, y = 0.0 and phase on entry = 0

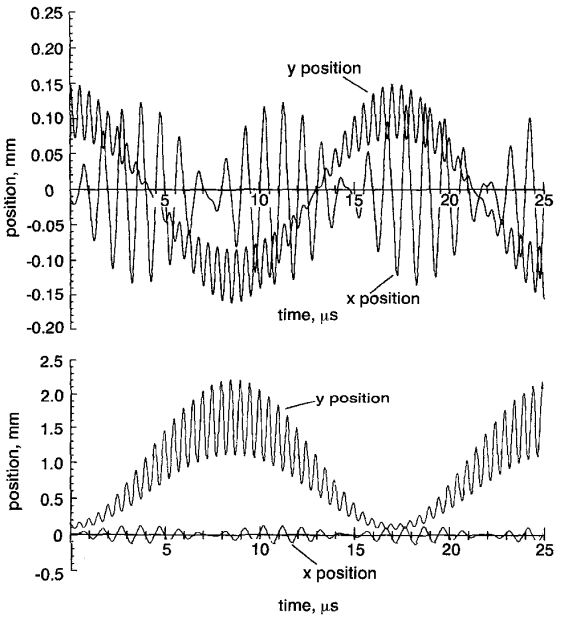

Fig. 5 *Numerical simulation of ion trajectories in x and y for Ar^+ without $\boldsymbol{B}$ (upper trace) and with $\boldsymbol{B}$ (lower trace)*
Point of entry in both cases: x = 0.01 mm, y = 0.15 mm and phase on entry = 0

y = 0.15mm and the AC phase on entry is 0. It is important to note that the scales of the upper ($\boldsymbol{B}$ = 0) and lower traces are different by a factor of 10. The magnetic field has no effect on ion motion in the x-direction; however, ion motion in the y-direction is both displaced and increased in amplitude from 0.3mm peak-to-peak to 2mm peak-to-peak. In Fig. 6 the ion originates at x = 0.01mm, y = 0.15mm but the AC phase on entry this time is 1 rad (i.e. the ion does not enter when the AC is at a zero crossing). The y oscillations with $\boldsymbol{B}$ = 0 (upper trace) are larger than

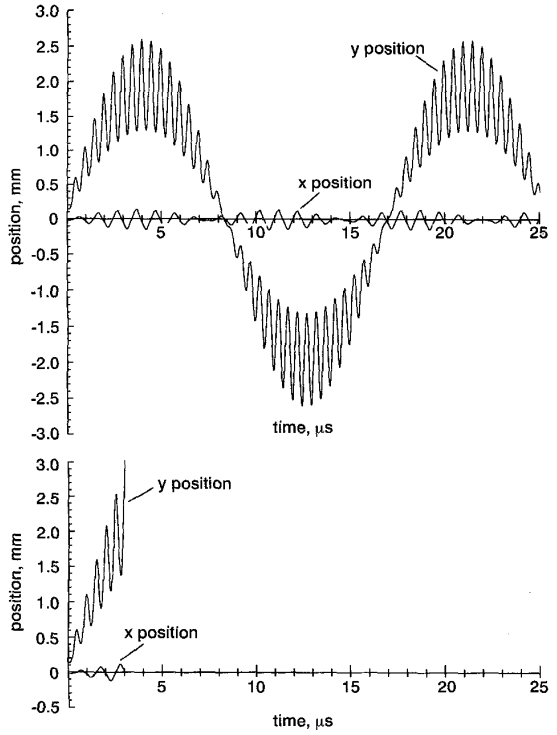

Fig. 6 *Numerical simulation of ion trajectories in x and y for Ar^+ without **B** (upper trace) and with **B** (lower trace)*
Point of entry in both cases: x = 0.01 mm, y = 0.15 mm and phase on entry = 1 rad

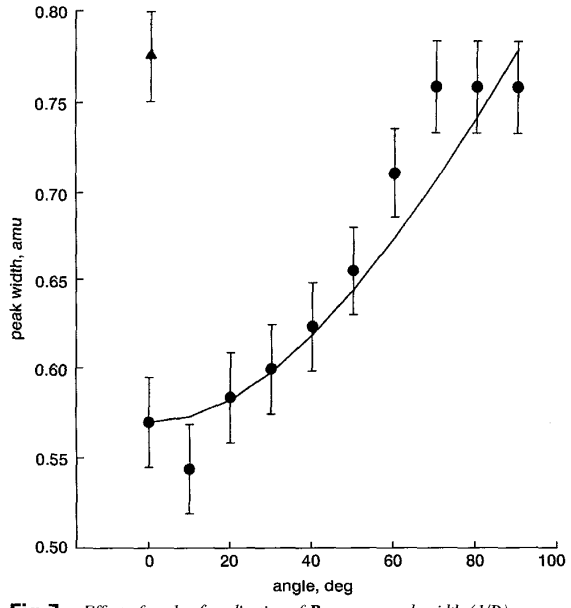

Fig. 7 *Effect of angle of application of **B** on mass peak width (1/R)*
● with **B**-field
▲ without **B**-field
—— cos θ fit

in Fig. 5, and application of the magnetic field displaces them so far that the ion quickly exceeds r_0 = 2.6mm and the ion is lost (lower trace). We note again that motion in the x-direction parallel to the field) is unaffected: it is ion motion in the y-direction (perpendicular to the field) which is modified.

3.2 Effect of angle of applied magnetic field

As a further experimental check on the hypotheses (i) and (ii), the angle of application of the field with respect to the x-axis was varied. Fig. 7 shows the peak width ΔM of mass 40 spectra as the angle of application of the magnetic field, θ, is varied from 0 to 90° in successive steps of 10° with mass spectra being taken at each step. Clearly there is little effect on the resolution as the magnetic field is applied in one direction and the maximum effect of $\boldsymbol{B}$ is applied perpendicularly, supporting both the previous hypotheses and the theoretical interpretation. The solid line shows a cosine (θ) fit to the data. This is to be expected if, as postulated, it is the component of the magnetic field in the x-direction which is responsible for the observed resolution enhancement.

4 Conclusions

Experimental results for a 5 inch QMS have been presented showing the effect of a static, transverse magnetic field applied across the mass filter. Enhanced resolution and ion transmission for a given operating condition (U/V ratio) is observed for Ar^+ spectra. It is believed that the increased ion transmission is due to coupling of magnetic leakage flux into the ion source, resulting in increased numbers of ions being injected into the mass filter. The increase in resolution is ascribed to the modification of ion motion in the mass filter by the magnetic field. The mass spectra with and without the magnetic field applied have been successfully modelled by computing the trajectories for large numbers of ions injected uniformly into the mass filter. All ions entering the QMS mass filter with trajectories not parallel to the direction of the applied magnetic field will experience an additional force, which modifies their motion. This results in rejection of ions in the low-mass tail of the mass spectrum, giving increased resolution for a given set of DC and AC operating conditions. This conclusion is supported by an experiment by which the angle of application of the magnetic field was varied in the x–y plane.

5 References

1 DAWSON, P.H.: 'Quadrupole mass spectrometry and its applications' (AIP, New York), 1995
2 TAYLOR, S., TUNSTALL, J.J., LECK, J.H., TINDALL, R.F., JULLIEN, J.P., BATEY, J., SYMS, R.R.A., TATE, T., and AHMAD, M.M.: 'Performance improvements for a miniature quadrupole with a micromachined mass filter', *Vacuum*, 1999, **53**, (1–2), pp. 203–206
3 HOLKEBOER, D.H., KARANDY, T.L., CURRIER, F.C., FREES, L.C., and ELLEFSON, R.E.: 'Miniature quadrupole residual gas analyzer for process monitoring at milliTorr pressures', *J. Vac. Sci. Technol. A, Vac. Surf. Films*, 1998, **A16**, (3), pp. 1157–1162
4 REUBEN, A.J., SMITH, G.B., MOSES, P., VAGOV, A.V., WOODS, M.D., GORDON, D.B., and MUNN, R.W.: 'Ion trajectories in exactly determined quadrupole fields', *Int. J. Mass Spectrom. Ion Process.*, 1996, **154**, pp. 43–59
5 MUNTEAN, F.: 'Transmission study for rf only quadrupoles by computer simulation', *Int. J. Mass Spectrom. Ion Process.*, 1995, **151**, pp. 197–206
6 ZHAOHUI, D., and DOUGLAS, D.J.: 'Peak splitting with a quadrupole mass filter operated in the second stability region', *J. Am. Soc. Mass Spectrom.*, 1999, **10**, pp. 1263–1270
7 BLAUM, K., GEPPERT, CH., MÜLLER, P., NÖRTERSHÄUSER, W., OTTEN, E.W., SCHMITT, A., TRAUTMANN, N., WENDT, K., and BUSHAW, B.A.: 'Properties and performance of a quadrupole mass filter used for resonance ionization mass spectrometry', *Int. J. Mass Spectrom. Ion Process.*, 1998, **181**, pp. 67–87

8 BATEY, J.H.: 'Quadrupole gas analysers', *Vacuum*, 1987, **37**, pp. 659–668
9 MA, F.M., and TAYLOR, S.: 'Simulation of ion trajectories through the mass filter of a quadrupole mass spectrometer', *IEE Proc. Sci. Meas. Technol.*, 1996, **143**, (1), pp. 71–76
10 VOO, A.C.C., NG, R., TUNSTALL, J.J., and TAYLOR, S.: 'Transmission through the quadrupole mass spectrometer mass filter: the effect of aperture and harmonics', *J. Vac. Sci. Technol. A, Vac. Surf. Films*, 1997, **15**, (4), pp. 2276–2281
11 GIBSON, J.R., TAYLOR, S., and LECK, J.H.: 'Detailed simulation of mass spectra for quadrupole mass spectrometer systems', *J. Vac. Sci. Technol. A, Vac. Surf. Films*, 2000, **A18**, (1), pp. 237–243
12 PORITSKY, H., and GERRARD, J.P.: 'An integrable case of electron motion in electric and magnetic field', *J. Appl. Phys.*, 1952, **23**, (8), pp. 928–930
13 PAVLENKO, Y.G., and TOPOROBA, A.N.: 'New Mass spectrometer quadrupole in a magnetic field', *Radiotekh. Electron.*, 1996, **41**, pp. 508–512
14 TUNSTALL, J.J., TAYLOR, S., VOURDAS, A., LECK, J.H., and BATEY, J.: 'Application of a static magnetic field to the mass filter of a quadrupole mass spectrometer', *Vacuum*, 1999, **53**, (1-2), pp. 211–213

6 Appendix

Eqns. 1–3 have been written in a dimensionless form where the only dimension that appears is that of length displacement.

Time $t = 2\xi/\omega$; angular frequency $\omega = 2\pi f$. U is the direct potential; V is the alternating potential amplitude;

$$a = \frac{4eU}{m\omega^2 r_0^2} \qquad q = \frac{2eV}{m\omega^2 r_0^2}$$

m is the mass of the ion; r_0 is the inscribed radius of QMS. The components of the magnetic field $\boldsymbol{B}$ are

$$(b_1, b_2, b_3) = \left(\frac{2eB_x}{m\omega}, \frac{2eB_y}{m\omega}, \frac{2eB_z}{m\omega}\right)$$